Dynamical transitions and aging in the superdiffusive Pomeau-Manneville map

Samuel Brevitt[1,*] and Rainer Klages[1,†]

[1]*School of Mathematical Sciences, Queen Mary University of London, Mile End Road, London E1 4NS, UK*

The Pomeau-Manneville map is a paradigmatic intermittent dynamical system exhibiting weak chaos and anomalous dynamics. In this paper we analyse the parameter dependence of superdiffusion for the map lifted periodically onto the real line. From numerical simulations we compute the generalised diffusion coefficient (GDC) of this model as a function of the map's nonlinearity parameter. We identify two singular dynamical transitions in the GDC, one where it diverges to infinity, and a second one where it is fully suppressed. Using the continuous-time random walk theory of Lévy walks we calculate an analytic expression for the GDC and show that it qualitatively reproduces these two transitions. Quantitatively it systematically deviates from the deterministic dynamics for small parameter values, which we explain by slow decay of velocity correlations. Interestingly, imposing aging onto the dynamics in simulations eliminates the dynamical transition that led to suppression of the GDC, thus yielding a non-trivial change in the parameter dependence of superdiffusion. This also applies to a respective intermittent model of subdiffusive dynamics displaying a related transition.

I. INTRODUCTION

Diffusion is a fundamental feature of many dynamical systems in nature, technology and society [1]. In physics the interplay between diffusion on a large scale, and the random motion of particles on a smaller one, has been well-studied ever since the rise of thermodynamics and statistical mechanics [2, 3]. In many such diffusive processes, like Brownian motion, it is observed that the mean square displacement (MSD) of a diffusing particle increases linearly with time, $\langle x^2 \rangle \sim t$. However it is also observed in many natural processes that the MSD may instead increase as t^β, where β can be lesser (called *subdiffusion*) or greater (*superdiffusion*) than unity (*normal diffusion*). Such observations of anomalous diffusion are found in fields as diverse as physics, microbiology, chemistry and finance [4–10].

In parallel to this, the development of chaos theory led to an interest in the pseudo-stochastic and diffusive properties of deterministic chaotic dynamical systems [11–17]. The simplest examples are random walks on the line generated by deterministically chaotic one-dimensional maps, introduced and studied in pioneering works at the beginning of the 1980s [18–20]. Since then their diffusive dynamics have been widely explored by many different methods, such as stochastic theory [18–34]. periodic orbit theory [35–39], thermodynamic formalism [40, 41] and transfer operator techniques [26, 29, 42–44]. In these maps many irregular behaviours can be observed, like fractal parameter dependencies of transport coefficients [16, 26, 32, 42, 43], transitions to weak chaos (a subexponential separation of trajectories from nearby initial conditions, resulting in a Lyapunov exponent of zero [45–47]) and intermittency (periods of chaos punctuated by periods of laminar flow [48–50]) yielding different types of diffusion, which make them useful models for a variety of natural systems.

One important class of low-dimensional, time-discrete maps is the Pomeau-Manneville (PM) map, first constructed in order to study the chaos observed in turbulent flows in continuous-time Lorenz systems [48–50]. The map can be defined by

$$x_{n+1} := M(x_n) \quad \text{for} \quad M(x) := x + ax^z \ (\text{mod } 1) \qquad (1)$$

depending on parameters $a > 0$ and $z \geq 1$ for $0 \leq x \leq 1$, where x_n is the position of a point at discrete time $n \in \mathbb{N}$. This map has an unstable marginal fixed point at 0 which for certain ranges of the nonlinearity parameter z is known to produce intermittency and weak chaos [45, 48]. By symmetry and translation, this map can be extended across the real line to produce a map exhibiting either subdiffusion or superdiffusion by careful positioning of the fixed point [21, 24, 36, 40].

For the subdiffusive extension of the PM map (1), the time-scaling of the MSD and its dependence on the nonlinearity parameter z have been determined by different methods [21, 24, 25, 28, 31–33, 36–38, 40]. The associated generalised diffusion coefficient (GDC), however, which is the multiplicative constant in front of the MSD, has been calculated only rarely [37, 38]. Its full dependence on the two control parameters a and z has been reported in [32, 33], where computer simulation results were compared with analytic approximations obtained from continuous-time random walk (CTRW) theory. It was shown that under variation of z the GDC is fully suppressed right at the transition from normal to subdiffusion.

There also exist results for the time-dependent MSD of the superdiffusively extended PM map [22–25, 36, 40, 44]. These studies revealed that as the nonlinearity parameter increases, the map transitions through three different regimes of diffusion, i.e., from normal ($\beta = 1$) to superdiffusion ($1 < \beta < 2$) to ballistic motion ($\beta = 2$). The full parameter dependence of the associated GDC has been investigated only more recently. Reference [51] focused on the dependence of the GDC on a while [51, 52] reported simulation results for the GDC under variation of z, indicating an interesting transition scenario that, however, was not understood in terms of any theory.

In this article we investigate how the GDC of the superdiffusive PM map changes under variation of the nonlinearity parameter z. Our paper is organised as follows. After introducing the superdiffusive extension of the PM map at the beginning of Sec. II, we briefly review the corresponding stochastic (Lévy walk) model formulated in terms of CTRW theory.

* s.brevitt@qmul.ac.uk
† r.klages@qmul.ac.uk

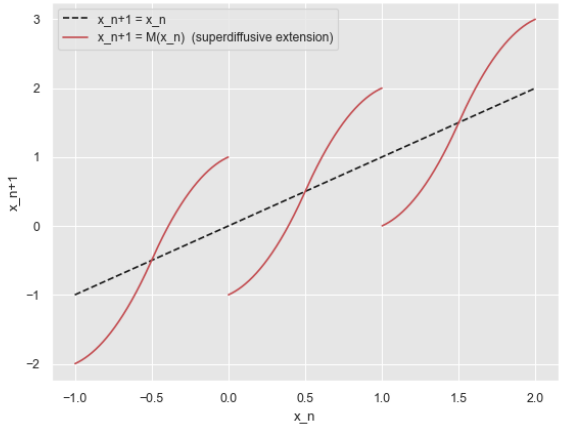

Figure 1. The superdiffusive extension of the Pomeau-Manneville map for the case $z = 2$ (solid, red online). In black (dashed) is also shown the line $x_{n+1} = x_n$ for comparison.

We discuss the numerical data analysis and also outline an approach to approximate the GDC via a Taylor-Green-Kubo (TGK) expansion. In Sec. III we compare the superdiffusion obtained from the Lévy walk with the one generated by the map by calculating the GDC as a function of the nonlinearity parameter analytically, as well as from simulations. We provide a detailed analysis of the different diffusive regimes, and the transitions between them. In Sec. IV we explore the effect of aging on the GDC and compare our superdiffusive results with an analogous study of subdiffusive dynamics generated by the PM map. We conclude with a brief summary in Sec. V.

II. DETERMINISTIC AND STOCHASTIC MODELLING

The version of the map we will consider is the same as the one studied in [24, 25, 36, 40, 51, 52],

$$M(x) = x + (2x)^z - 1 \quad \text{for} \quad 0 < x < \frac{1}{2} \quad , \qquad (2)$$

extended across the real line by $M(-x) = -M(x)$ and $M(x+1) = M(x) + 1$. In this paper we will only concern ourselves with the z-dependence of the map. Implicitly we have chosen a variable prefactor of $a = 2^z$ which ensures the height (the distance outside of the unit box that the map extends) remains fixed at 1. The subtracted unit guarantees the marginal fixed point is located at the boundary of each branch (see Fig. 1). We note that the a-dependence of the diffusion in the map is studied in depth in [51]. At $z = 1$, the map reduces to a piecewise linear one, the dynamics of which are well understood [16, 26, 27, 29, 53]. Increasing the parameter z increases the extent to which the map clings to the fixed point.

Anomalous diffusion in this type of deterministic dynamical systems has often been modelled stochastically by CTRWs [21–24, 31, 32]. A CTRW is a type of random walk in which both the vectors of displacement, and the time interval between displacement events, are drawn randomly from a defined joint distribution; see [4, 6, 7, 10, 54] for reviews. It is well studied partly due to the existence of a simple closed-form expression in Fourier-Laplace space for the propagator of such a random walk, via the Montroll-Weiss equation [55–57], from which key statistics such as the MSD can be easily extracted. The model used in [23–25, 32, 33] approximates the time spent by a particle in the laminar phase of motion near the fixed point as being distributed according to the power law (Pareto distribution)

$$w(t) = \frac{\gamma b^\gamma}{(b+t)^{1+\gamma}} \qquad (3)$$

for $\gamma := 1/(z-1)$ and $b := \gamma/a$. This distribution is generated from the map by the following reasoning: The time taken for a particle to escape the fixed point, given an initial injection point, is found by modelling the laminar motion away from the fixed point as a continuous process in time, using the map to generate a differential equation which can be easily solved. The distribution of waiting times follows by assuming a uniform injection density.

Since in the superdiffusive extension of the map, such periods correspond to a ballistic motion of (near-)integer jumps, the referenced literature supposes the jump lengths to correspond exactly to the interval times according to a constant velocity [22, 24],

$$p(\ell \,|\, t) = \frac{1}{2}\,\delta(|\ell| - v_0 t) \quad , \qquad (4)$$

where we enable the particle to move either left or right along a one-dimensional axis with equal probability. These choices define the model as a *Lévy walk* [10, 58–60]. When a particle is trapped near the fixed point, the map transports it (almost) exactly one unit in space per timestep. Hence here we opt to take $v_0 \equiv 1$, which yields an upper bound for the map's exact velocity. From (3) and (4) the joint density

$$\psi(x,t) = w(t)\, p(x \,|\, t)$$

follows. We also assume that, along the course of a single trajectory, the particle moves continuously with constant speed between its original position and its destination. There are alternative models in which a particle is supposed to wait in one location for a random time before making an instantaneous jump of a corresponding distance, which require a different mathematical treatment [10, 24, 54]. These choices are substituted into the appropriate Montroll-Weiss equation [10, 24, 54],

$$\hat{\tilde{P}}(k,s) = \mathrm{Re}\left\{\frac{1-\tilde{w}(s+\mathrm{i}v_0 k)}{s+\mathrm{i}v_0 k}\right\}\frac{1}{1-\hat{\tilde{\psi}}(k,s)},$$

where $P(x,t)$ is the spatial density of the random walk as a function of time, and (k,s) are the respective Fourier- and Laplace-transformed variables for (x,t) (such transformations are indicated by $\hat{}$ and $\tilde{}$ respectively). The Laplace-transformed MSD can then be found very easily by

$$\langle \tilde{x}^2(s) \rangle = \frac{\partial^2}{\partial k^2}\hat{\tilde{P}}(k,s)\bigg|_{k=0} \quad , \qquad (5)$$

where an inverse transform is required to obtain the original quantity. Frequently in practice we find such transforms are intractable and instead we rely on asymptotic analysis to obtain the desired quantities to leading order only. The GDC [7, 32, 33] can then be defined by

$$K(z) := \lim_{t\to\infty} \frac{\langle x^2\rangle}{t^\beta} \tag{6}$$

for the appropriate $\beta > 0$ wherever this limit exists. A more detailed derivation of the appropriate formulae can be found in the Appendix, based on methods described in [24, 33, 52].

Numerical estimates for $K(z)$ were generated in two ways: The naïve approach is to take a large ensemble of particles, generated from uniformly random initial conditions; generate from each a trajectory, for some long amount of time; and periodically measure and calculate the MSD at different times. The desired coefficient $K(z)$ can then be found by matching a curve of the form $\langle x^2\rangle \sim Kt^\beta$, e.g., by fitting a linear regression on a log-log plot, where $\log\langle x^2\rangle \sim \beta \log t + \log K$. However, care must be taken in choosing which points in time to sample, and how to appropriately handle transient behaviour.

Similar analyses were done in [51, 52]. But the method we will use for the remainder of this paper is derived from the TGK formula [14, 61, 62] for calculating the MSD. This approach uses correlations between 'velocities' – which, here in a time-discrete setting, we take as displacements between timesteps – to produce an exact summation formula for $\langle x^2\rangle$ [30, 33, 53, 63]. A particular advantage is that this summation can be broken down into its constituent parts to analyse the effects of higher-order correlations, as we will do in Sec. III. Another advantage is that in general we found this method to be more computationally efficient than estimating the MSD directly by fitting a curve, in terms of the quality of the results generated. The method works as follows: By considering

$$x_t - x_0 = \sum_{k=0}^{t-1} v_k$$

we produce the expansion [14, 61, 62]

$$\begin{aligned} K(z) &:= \lim_{t\to\infty} \frac{1}{t^\beta}\langle (x_t - x_0)^2\rangle \\ &= \lim_{t\to\infty} \frac{1}{t^\beta} \sum_{k=0}^{t-1}\sum_{l=0}^{t-1} \langle v_k v_l\rangle \\ &= \lim_{t\to\infty} \frac{1}{t^\beta} \left[\sum_{k=0}^{t-1}\langle v_k^2\rangle + 2\sum_{k=0}^{t-1}\sum_{j=1}^{t-k-1}\langle v_k v_{k+j}\rangle\right] . \end{aligned} \tag{7}$$

For analysing the impact of correlations captured by the second term, it is advisable to consider only the integer part of each x_k, and neglect the fractional part, which drops out for $t \to \infty$ thus giving the same asymptotic result either way [30, 53]. This choice ensures that the first term can be understood as a simple random walk result that, for the present setting, correctly reproduces the exact value of $K(1) = 2/3$, thus giving a physically meaningful lowest order approximation [27, 30, 53].

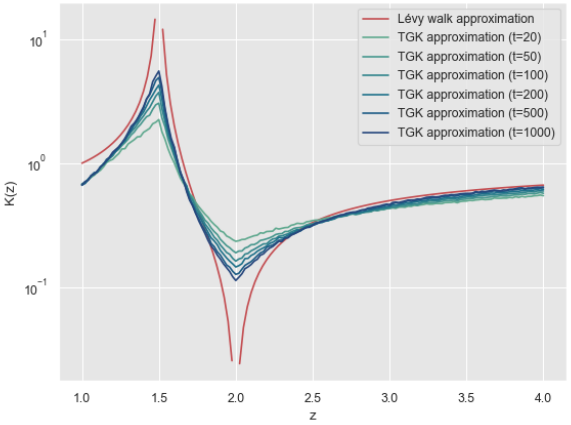

Figure 2. The GDC $K(z)$ (6) generated from TGK expansions (7) of the superdiffusive PM map (2), using increasingly many terms t of the expansion and the analytic estimate for β obtained from (8) (rough curves, t increasing from light to dark). Also shown is the Lévy walk approximation (6), (8) (smooth curve, red online). All plots are generated from an ensemble of 10^4 particles and consist of 151 points.

III. RESULTS

Using (5) gives us (to leading order) the MSD

$$\langle x^2\rangle \sim v_0^2 \begin{cases} \frac{2b}{\gamma-2}\, t, & 1 < z < \frac{3}{2} \\ \frac{2b^{\gamma-1}(\gamma-1)}{(3-\gamma)(2-\gamma)}\, t^{3-\gamma}, & \frac{3}{2} < z < 2 \\ (1-\gamma)\, t^2, & z > 2 \end{cases} . \tag{8}$$

Explicit calculations of these results can be found in the Appendix, based on methods described in [24, 33, 52]. While the time-dependence on t^β is very well known [23–25, 28, 31–33, 36–38, 40], the multiplicative constant yielding the GDC, according to (6), has only been reported more recently within the context of higher-dimensional Lévy walks, cf. the suppemental material of [64]. There the direct one-dimensional derivation detailed in our Appendix was not discussed. We now match the GDC $K(z)$ from (8) to results obtained numerically from the map itself. These analytic results are shown in Fig. 2, along with numerical estimates of the same quantity calculated via the TGK formula.

We see from the generated formulae that the parameter space of z is divided into three distinct regimes, at the boundaries of which $K(z)$ ceases to be continuous as a function of z, and $\beta(z)$ ceases to be differentiable: (I) where $1 < z < \frac{3}{2}$, for which the diffusion is normal ($\beta = 1$); (II) where $\frac{3}{2} < z < 2$, for which superdiffusion is observed ($1 < \beta < 2$); and (III) where $z > 2$, for which an extreme form of ballistic superdiffusion is observed ($\beta = 2$). These emerge from the calculations as a direct result of moments of the waiting time distribution $w(t)$ ceasing to exist due to heavy tails: in (I), where $\gamma > 2$, $w(t)$ has a well-defined mean and variance and so the Central Limit Theorem dictates the diffusion to be normal

and with (in the long time limit) a Gaussian propagator; in (II), $1 < \gamma < 2$ and therefore $w(t)$ has a first moment but not a second, resulting in anomalous diffusion; in (III), $0 < \gamma < 1$ and therefore not even a first moment exists for $w(t)$, resulting in ballistic trajectories of unbounded average length.

At the dynamical transition points $z = 3/2$ and $z = 2$, we observe in the case of the Lévy walk that $K(z)$ approaches infinity and zero respectively. This is because, considering a more detailed expansion, via the same methodology, we calculate (in agreement with known results [23, 24])

$$\langle x^2 \rangle \sim \begin{cases} t \log t, & z = \frac{3}{2} \\ t^2 / \log t & z = 2 \end{cases} , \tag{9}$$

which matches to exact results for the PM map obtained by methods of dynamical system theory [36, 40, 44]. Fig. 2 shows that around these two transition points $K(z)$ displays characteristic shapes. Numerical estimates with finite computation time cannot overcome the slow logarithmic corrections of (9) to reproduce these analytical predictions accurately. But taking increasingly many terms t from the TGK expansion (which equates to looking at the process over a longer time) indeed produces sharper peaks and troughs at the dynamic transitions (see Fig. 2), thus confirming the Lévy walk scenario at least qualitatively.

We remark that the corresponding subdiffusive PM map exhibits a transition from normal to subdiffusion in the GDC, whose shape is somewhat related to the one from superdiffusion to ballistic of the superdiffusive map at $z = 2$, in the sense that $K(z)$ is also fully suppressed by converging to zero [32, 33]; see Fig. 5 bottom right. This subdiffusive suppression matches to the result $\langle x^2 \rangle \sim t/\log t$ [21, 24, 25, 28, 31–33, 36–38, 40]. In [33] it was shown analytically by means of CTRW theory that logarithmic terms survive up to long crossover times at parameter values next to this transition point thus characterising the whole transition scenario. Equation (9) and Fig. 2 suggest that respective logarithmic time dependencies shape the two transitions in $K(z)$ of the superdiffusive case as well. We note, however, that the divergence to infinity at $z = 3/2$ is of a new type and very different from the one displayed by the subdiffusive model.

The assumption that the particle 'walks' between locations with constant velocity, rather than waiting in one location before making an instantaneous 'jump' as was assumed in the subdiffusive case in [33], turns out to be especially important: We find in regime (I) exhibiting normal diffusion that the resulting $K(z)$ is by our calculation identical in both models, but in regimes (II) and (III) exhibiting superdiffusion, the 'jump' and 'walk' models (or 'jump' and 'velocity' models, as they were called in [24]) produce differing results. This is essentially because the heavy tails that appear above $z > 3/2$ mean that the particles currently on 'long' trajectories at a given point in time have enough of an influence for their position to affect the overall average MSD to leading order. We find the 'walk' (or 'velocity') model to be more appropriate in this instance, both in the sense of the justification from first principles, and in the matching to the concrete numerical results. An outline of the different models and the differences between them can be found in [10, 24, 54].

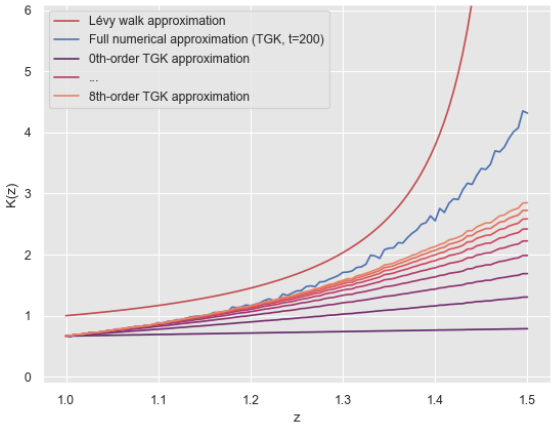

Figure 3. $K(z)$ generated from TGK expansions (7) of the superdiffusive PM map, using increasingly many orders of correlation terms $\langle v_k v_{k+j} \rangle$ (lower rough curves, m increasing from dark to light). Also shown are the Lévy walk approximation (8) (uppermost smooth curve, red online) and the full TGK expansion (uppermost rough curve, blue online). All TGK plots are taken using 200 terms of a TGK expansion from an ensemble of 10^4 particles and consist of 101 points.

We now elaborate on the shape of $K(z)$ in the three different diffusive regimes. We observe a convergence in regime (III) when $z > 2$ towards the curve generated from the Lévy walk, as further discussed in Sec. IV. Likewise, our numerics indicates convergence to the Lévy walk result in regime (II) for $3/2 < z < 2$. However, for regime (I) in $0 < z < 3/2$ we notice a significant discrepancy, which relates to the limit of $K(z)$ as $z \to 1$. It is given by the stochastic Lévy walk calculations as $K(1) = 1$, but is shown numerically to have the value approximately $2/3$. Since for $z = 1$ the function $M(x)$ reduces to a linear shift map, the true value can also be calculated via straightforward analytic means to be $K(1) = 2/3$, matching to a simple random walk result [26, 27, 29, 30, 53]. This is not desperately surprising, since it was also shown in the subdiffusive case that in the regime of normal diffusion, for $z < 3/2$, the Lévy model is invalid [33] and instead a selectively constructed random walk was used to match $K(z)$ in this regime. A normally-diffusive CTRW with exponential waiting times was also applied and found to match sufficiently well in this regime. Somewhat surprisingly, in the superdiffusive case we were unable to identify any natural parameters of the system to fit an exponential walk process to match the numerical results. We were also unable to construct any appropriate random walks that could reproduce the general qualitative behaviour of $K(z)$ for $z < 3/2$, and particularly the correct asymptotic behaviour as $z \to 1$. Likewise an effort was made to refine the model by selectively adjusting the velocity parameter v_0 as a function of z, but this also failed to produce suitable results.

One clue as to why can be obtained from the breakdown of the TGK approximation described in Sec. II. In Fig. 3 we show the same expansion, with a fixed time parameter of

$t = 200$, focusing on the region $1 < z < 3/2$, reproduced at a higher resolution, along with a series of increasing partial expansions, starting with the '0th' order expansion featuring only the first of the two terms in (7), and sequentially adding cross-correlations from the second term of the formula (we call the 'mth' order expansion that in which j is allowed to range from 1 to m; i.e., correlations between displacements up to m time units apart are considered). This breakdown immediately shows us the problem with modelling the process as a random walk: In an ordinary random walk, each timestep is of the same duration, but in the dynamics of the map we observe correlations between adjacent timesteps (e.g. if a particle is moving ballistically for one step, it likely continues to do so for a longer sequence of steps). If, in the TGK expansion, we do not consider correlation terms, and only take the average squared integer velocity of a particle, we obtain a diffusion coefficient which gives the correct limit at $z = 1$ (in which case the map can be modelled exactly by a simple random walk) but is very slowly increasing for $z > 1$, as shown in Fig. 3. If we add correlations of higher and higher orders we obtain a steeper rise (while retaining the correct limit), but the convergence to the numerical results is slow, especially for larger $z < 3/2$. This shows that, especially for larger z, correlations of higher and higher orders are critical to the dynamics of the map, and explains why a simple random walk model is inappropriate.

Alternatively we may construct a random walk to account for low-order correlations between iterations of the map by looking at the average dynamics not just of $M(x)$ but of $\frac{1}{n}M^n(x)$ for $n > 1$. We consider the displacement of a particle after n steps (again taking only the integer part), and to initialise our points x_0 it would be sensible to draw them from the microscopic (i.e. modulo an integer) invariant density of the map on $0 < x < 1$. Inspired by [65–68], which show the invariant density on the reduced map (1) to be asymptotic to $\tilde{\rho}(x) \propto x^{1-z}$, we initialise our points from

$$\tilde{\rho}(x) \propto x^{1-z} + (1-x)^{1-z}, \tag{10}$$

noting that since $z < 3/2$, this density is normalisable. Histograms from numerical simulations starting from a uniform density show this to be a good approximation of the invariant measure where it exists. The diffusion coefficients generated from these random walks, considered as a function of z, are similar to those generated from the partial TGK sums (we decline to show a figure). Again the simple random walk produces a very shallow rise with z, while considering higher lengths of correlations $\frac{1}{n}M^n(x)$ results in an increase which more closely matches numerical findings. But again for z close to the transition, unboundedly many n are required for a good approximation. This again confirms that high-order correlations are critical to understanding the dynamics in this regime.

This is also shown in studying the densities of the duration between turning points in realisations of the PM map, as depicted in Fig. 4. In the simple case $z = 1$, the duration between turning points is as expected exponentially distributed, indicated by a straight line on a log-frequency axis. For $z > 3/2$ this develops into a (truncated) power law, indicated by a straight line on a log-log plot; but we see that even in the region $1 < z < 3/2$ of normal diffusion there is an immediate appearance of very long trajectories, and the curve evidently ceases to be purely exponential. Care should be taken to observe in the plot both the change in the qualitative shape of the distribution and the quantitative values – observe that the scale on the time axis includes some exceptionally large values even for small z well within the regime of normal diffusion, and the line on the semi-log plot ceases to be straight. Overall this analysis reveals a very gradual transition from a *pure* exponential law at $z = 1$ to a *pure* power law for $z > 2$, rather than a clean dynamical transition as one might expect, and explains why the attempted fitting of an exponential CTRW law, as was achieved in [33], failed for the superdiffusive map. The distinction between this superdiffusive model and the subdiffusive map in [32, 33] is now clear: For the subdiffusive map, the laminar stage of the motion corresponded to times at which a point was near-stationary and did not 'jump'. And the jumps themselves were of unit length and random direction, uncorrelated from the direction of previous jumps, making them easier to approximate with a suitable random walk or other normally-diffusive process. For the superdiffusive map, these periods of long laminar motion correspond to motion in a single direction, which introduces the very problems we observe.

IV. EFFECT OF AGING ON THE GENERALISED DIFFUSION COEFFICIENT

Finally we explore the consequences of aging for numerical estimates of $K(z)$. In the present setting, aging denotes the dependence of the MSD, and hence of $K(z)$, on the duration, or aging time, between the initialisation of the system dynamics and the start of the actual measurement [31, 65, 69–71]. Up to this point all estimates have been taken commencing from a uniform density. But since we interest ourselves in the behaviour occurring in a long time limit, and transient dynamics slow our ability to produce accurate calculations, a reasonable suggestion is to allow a degree of relaxation towards the invariant density to take place before beginning measurements, to reduce the effect of transient behaviour on estimates. This is also a reasonable thing to suppose since many systems observed in nature typically evolve for a long time before human measurement of them can commence. However, we present here results for the GDC which indicate that some caution is necessary.

In Fig. 5 we apply varying degrees of aging to an ensemble of particles before calculating $K(z)$ via a TGK expansion. We also show the same calculations starting from the (approximate) invariant density (10) where it exists for $z < 2$, and for $z \geq 2$ the delta function on $\{0, 1\}$, the only existing normalisable density in this region. We see that the non-aged results match fairly well with the Lévy walk model, as was already observed in Fig. 2. But as the aging time increases they converge to the result from the invariant density, and the constant function $K(z) = 1$, which is trivially the exact result if points are initialised on the fixed points, respectively. While

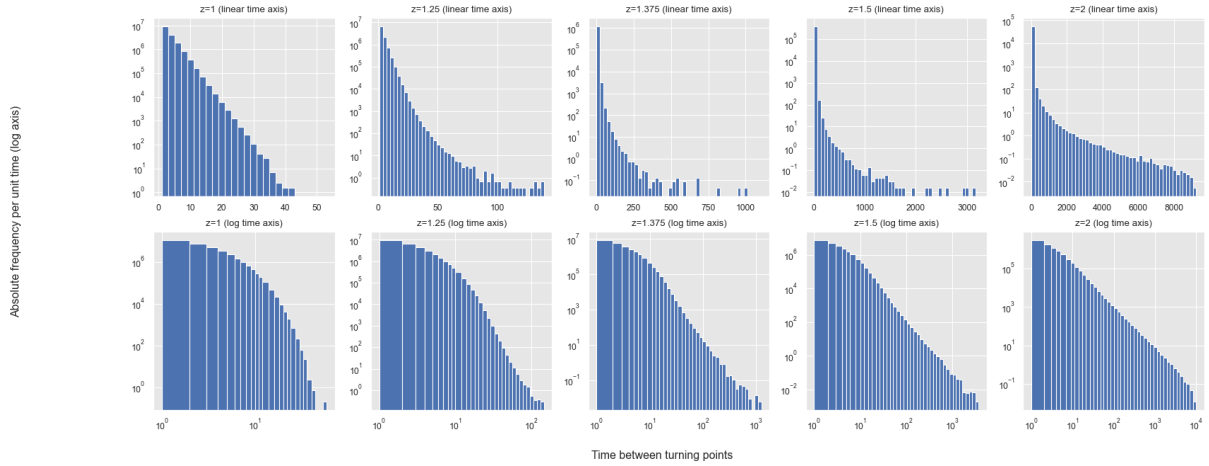

Figure 4. Histograms of the duration between turning points in trajectories of the PM map, for five different values of z. For each plot, an ensemble of 10^4 particles drawn from a uniform distribution was put through 10^4 iterations of the map, and each trajectory was split at its turning points into periods of monotone motion, the time duration of which is histogrammed here. Histograms are shown on a log-frequency (top) and log-log (bottom) axis and consist of a variable number of bins not exceeding 50, with each bin representing a variable number of data values in order to keep the bar widths relatively even. The height of each bar is rescaled in accordance with the number of data values it represents.

for $z < 3/2$ in regime (I) the GDC is not visibly affected by the aging, for $z > 3/2$ in regimes (II) and (III) the aged results are very different from the familiar non-aged curve. We note that the limit of these results, the curve corresponding to the invariant density, does not exhibit any at all of the logarithmic corrections discussed previously at $z = 2$ which lead $K(z)$ to almost vanish.

The cause of this effect – the uniform raising of the $K(z)$ curve visible for $z > 3/2$ – is due to the fact that the aged densities feature a more concentrated accumulation near the endpoints, which would lead to increased correlations in the short term as more particles are in the ballistic phase of motion. This effect is in principle observed for all ranges of the parameter z, but is only prominent in the regions where trajectories are especially long, and where the invariant density to which the aged densities are converging is especially peaked at the endpoints; namely, $z > 3/2$. The disappearance of logarithmic corrections at $z = 2$ is also easily explained, since around that transition, the initial density is very close to the delta function, and so almost all particles are on long trajectories for most or all of the entire measurement period, resulting in $K(z) \approx 1$.

That apart from a trivial transient there is no effect of aging on $K(z)$ in regime (I) for $z < 3/2$ was to be expected: A normalisable invariant density exists for the microscopic ensemble, the system is ergodic, and any initial density converges exponentially to the invariant one over time. In contrast, it is known that for $z \geq 2$ the PM map no longer has a normalisable invariant density, is only weakly ergodic [8, 47, 65], and therefore undergoes aging [33, 47, 65–67]. This implies that for our model all particles are eventually almost surely trapped around the fixed points corresponding to ballistic trajectories of length which is for each particle finite, but on average infinite. Interestingly, $K(z)$ ages even in the intermediate superdiffusive regime (II), $3/2 < z < 2$, where a normalisable invariant density still exists. This probably reflects what has been discussed for Lévy walks as ultraweak ergodicity breaking in that parameter regime [72].

However we note that, much as in the 'non-aged' case, if we take a longer expansion, these effects disappear and we regain the familiar non-aged Lévy walk GDC curve (see the bottom left inset in Fig. 5), which confirms that the method of preaging the ensemble is legitimate. In other words we have two conflicting limits: In the limit of increasing measurement time t, for any fixed aging time t_a (essentially, from any fixed initial density, assuming such a density is sufficiently 'physical'), we see convergence to the Lévy curve in Fig. 2. But in the limit of increasing aging time t_a, keeping measurement time t fixed, we obtain the dark blue curve in Fig. 5. We note that there is some literature on weakly chaotic systems which handles this problem by keeping the ratio t/t_a fixed, eg. [65]. We also remark that, beginning from an aged density, in contrast to the non-aged case, for large z the estimates for $K(z)$ converge onto the Lévy walk curve *from above*, rather than from below, indicating further that this curve represents the correct, 'true' GDC for large z.

A similar effect is observed for subdiffusive dynamics. In the bottom right inset of Fig. 5 is shown an equivalent plot for the subdiffusive PM map used in [32, 33], with $a = 5$, mirroring Fig. 7 in that paper. The same phenomenon as in Fig. 5 is observed: above $z > 3/2$, aging begins to uniformly reduce $K(z)$ until it converges to the result from the invariant density, which in this case is $K(z) = 0$ for $z > 2$.

The result of all of this is to present a general principle: That, for measurements taken over finite time (respectively, for TGK expansions of finite length), it is, somewhat counter-

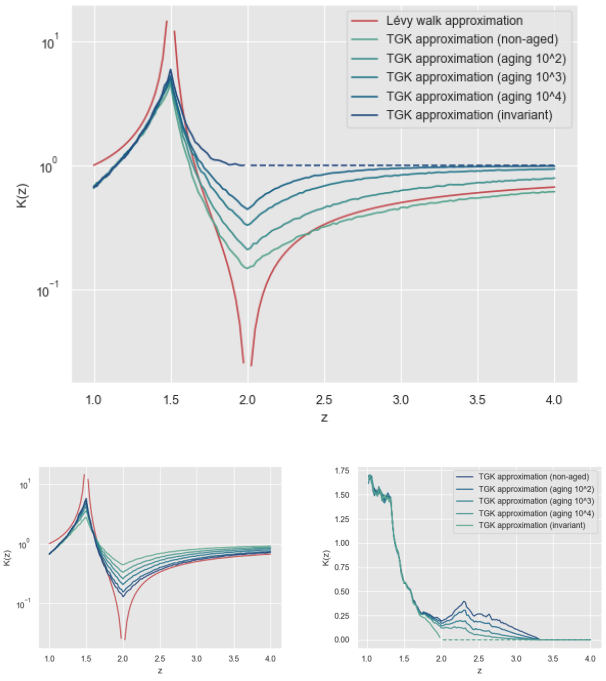

Figure 5. Top: TGK approximations of $K(z)$ for the superdiffusive PM map, starting from increasingly aged ensembles of particles initialised from a uniform density (aging duration increasing from light to dark), as well as starting from a normalisable invariant density (where it exists; darkest uppermost curve, blue online) or from a delta function (dashed line). Also shown is the Lévy walk approximation (smooth curve, red online). All TGK plots are taken using 200 terms of a TGK expansion from an ensemble of 10^4 particles and consist of 151 points (50 points in the case of the invariant ensemble). Bottom left: an identical plot to that shown in Fig. 2, initialised from an ensemble aged by 100 timesteps. Bottom right: an identical plot to that shown above, for the subdiffusive extension of the map studied in [33], mirroring Fig. 7 in that paper, with $a = 5$ fixed (aging duration increasing from dark to light, invariant curve shown at the bottom, in teal online).

intuitively, preferable to average one's ensembles over a uniform density, with all the transients that this necessitates, than from one closer to the more 'natural' invariant density. At least this applies to regimes (II) and (III) for $z > 3/2$. We see that in fact, results are in general 'better' this way, in the sense of reproducing the long-time limit Lévy walk curve, while for short sampling times, measuring from an aged or even invariant density can produce some very different results. Our exposition here supplies some numerical evidence to this principle.

V. CONCLUSION

In this article we conducted an analysis on a superdiffusive extension of the PM map. We calculated numerically the GDC of the map $K(z)$, as a function of the parameter of the map's nonlinearity, using TGK expansions, and produced a CTRW model in the form of a Lévy walk to stochastically model the map's dynamics, comparing the GDC generated by the model to the numerical results obtained from the map. We identified two non-trivial diffusive transitions in the dynamics, which represent themselves by discontinuities in $K(z)$: one for which $K(z)$ diverges, and one for which $K(z)$ is fully suppressed. Our Lévy walk model reproduces the numerically calculated $K(z)$ almost exactly, explaining the dynamical transitions through logarithmic corrections to the growth of the MSD, with the exception of a systematic quantitative deviation in the limit of normal diffusion. In this regime the dynamics are highly non-trivial and can partially be explained by high-order correlations between displacements of the map, which manifest in a much more subtle way than in the case of subdiffusion. Various numerical evidence is presented as part of this discussion.

We also investigated the effect of aging on the generated numerics. We find that, in the limit of increased aging, the suppression in $K(z)$ at the transition from superdiffusion to ballistic motion is eliminated, for finite measurement times, while the divergence at the other, from normal to superdiffusion, is preserved. This elimination is also reproduced in the case of the subdiffusive PM map. We identify this as a problem of conflicting limits as both aging time and measurement time go to infinity, which requires one to take caution when conducting numerical or even physical experiments. We state a general principle that uniform densities should be preferred to more 'natural' invariant ones if ergodicity of the dynamics is not ensured, a claim which is supported numerically.

It would be very interesting to test whether such dynamical transitions in the GDC, and associated aging effects, can be observed in experiments. As candidates we would be thinking of blinking quantum dots and cold atoms in atomic lattices, where features of anomalous diffusion, aging and weak ergodicity breaking have already been reported [73, 74]. It would also be worthwhile to explore theoretically the parameter dependence of generalised transport coefficients in other types of anomalous dynamical systems, such as stochastic generalised Langevin dynamics [5] and related deterministic chaotic models [75], which are known to generate a variety of different dynamical transitions.

VI. ACKNOWLEDGEMENTS

R.K. acknowledges first numerical results reported by Dominic Pegler and Alexander Schulz in their Master's theses that paved the way for the present work. R.K. is an External Fellow at the London Mathematical Laboratory.

Appendix A: Supplementary calculations

The aim is to construct a CTRW process with wait time distributed according to a density $w(t)$ and step length according to a density $p(x\,|\,t)$. $w(t)$ can be determined in the following way: Let t be a continuous variable representing the number of timesteps of the discrete process, then we allow ourselves

to use the approximation

$$\frac{\mathrm{d}x}{\mathrm{d}t} \simeq x_{n+1} - x_n = a x_n^z$$

for x near the fixed point. This, with initial condition $x(0) = x_0$, gives a differential equation with solution

$$x_t = [(at + C)(1-z)]^{\frac{1}{1-z}}$$

where C is a constant to be determined: at $t = 0$,

$$x_0 = [C(1-z)]^{\frac{1}{1-z}} \implies C = \frac{x_0^{1-z}}{1-z}$$
$$\implies x_t = \left[\frac{1}{x_0^{z-1}} - at(z-1)\right]^{-\frac{1}{z-1}}$$

This gives us an equation for the laminar motion of a point under these dynamics, depending on an initial point x_0. We suppose that a particle has 'escaped' the fixed point, and makes a jump, when it reaches $x_t = 1$, which occurs at time

$$1 = \left[\frac{1}{x_0^{z-1}} - a(z-1)t_{\mathrm{esc}}\right]^{-\frac{1}{z-1}}$$
$$\implies t_{\mathrm{esc}} = \frac{x_0^{1-z} - 1}{a(z-1)}$$

Thus the time distribution $w(t)$ is determined by this and the distribution of points going into the fixed point, the injection distribution $P_{\mathrm{in}}(x_0)$, which we assume to be uniform:

$$w(t) \simeq P_{\mathrm{in}}(x_0)\left|\frac{\mathrm{d}x_0}{\mathrm{d}t_{\mathrm{esc}}}\right|$$

Here we obtain from the above

$$x_0 = [a(z-1)t_{\mathrm{esc}} + 1]^{\frac{1}{1-z}}$$
$$\implies \frac{\mathrm{d}x_0}{\mathrm{d}t_{\mathrm{esc}}} = -a[(z-1)at_{\mathrm{esc}} + 1]^{\frac{z}{1-z}}$$
$$\implies w(t) = \left|\frac{\mathrm{d}x_0}{\mathrm{d}t_{\mathrm{esc}}}\right| = a[(z-1)at + 1]^{\frac{z}{1-z}}$$

Letting $\gamma = \frac{1}{z-1}$ and $b = \frac{\gamma}{a}$, we transform the above into

$$w(t) = \frac{\gamma b^\gamma}{(b+t)^{1+\gamma}}$$

which we see is the form of a Pareto distribution. To take the Laplace transform of this we can use the known result

$$\mathscr{L}\{(a+t)^\nu\} = s^{-\nu-1}\,\mathrm{e}^{as}\,\Gamma(1+\nu, as), \quad |\arg a| < \pi$$
$$\implies \tilde{w}(s) = \gamma(bs)^\gamma\,\mathrm{e}^{bs}\,\Gamma(-\gamma, bs)$$

for $\Gamma(z,x) = \int_x^\infty t^{z-1}\mathrm{e}^{-t}\,\mathrm{d}t$, the incomplete Gamma function. It is convenient to write this in the form

$$\tilde{w}(s) = 1 - (bs)^\gamma\,\mathrm{e}^{bs}\,\Gamma(1-\gamma, bs)$$

which can be obtained easily from a change of variable and integration by parts.

The displacement of the jump is specified to be proportional to the wait time in length and uniform in direction, i.e. our joint distribution is

$$\psi(x,t) = w(t)\,p(x\,|\,t) \quad \text{with} \quad p(x\,|\,t) = \frac{1}{2}\delta(|x| - v_0 t)$$

The Montroll-Weiss equation is then derived as follows: we define $Q(x,t)$ as the probability density to *arrive at* position x at *exactly* time t by the master equation

$$Q(x,t) = \int_{-\infty}^{\infty}\mathrm{d}x'\int_0^t \mathrm{d}t'\,Q(x-x', t-t')\,\psi(x',t') + \delta(x)\delta(t)$$
$$\implies \hat{\tilde{Q}}(k,s) = \hat{\tilde{Q}}(k,s)\,\hat{\tilde{\psi}}(k,s) + 1 = \frac{1}{1-\hat{\tilde{\psi}}(k,s)}$$

(the integral part of this equation is a straightforward continuity equation in the case a previous trajectory exists; the delta functions represent our initial condition that all trajectories start at $x = 0$ at $t = 0$) and so our main probability density of *being at* position x at time t is

$$P(x,t) = \int_0^t \mathrm{d}t'\int_{-\infty}^{\infty}\mathrm{d}x'\,Q(x-x', t-t')\,\Psi(x',t')$$
$$\implies \hat{\tilde{P}}(k,s) = \hat{\tilde{Q}}(k,s)\,\hat{\tilde{\Psi}}(k,s) = \frac{\hat{\tilde{\Psi}}(k,s)}{1-\hat{\tilde{\psi}}(k,s)}$$

where here $\Psi(t)$ defines the density of a particle part-way through a trajectory; here we take it as

$$\Psi(x,t) = p(x\,|\,t) \times \mathbb{P}[w(t) > t]$$
$$= \frac{1}{2}\delta(|x| - v_0 t)\int_t^\infty w(t')\,\mathrm{d}t'$$
$$\implies \hat{\tilde{\Psi}}(k,s) = \mathrm{Re}\left\{\frac{1-\tilde{w}(s+\mathrm{i}v_0 k)}{s+\mathrm{i}v_0 k}\right\}$$

[54] and our master equation becomes

$$\hat{\tilde{P}}(k,s) = \mathrm{Re}\left\{\frac{1-\tilde{w}(s+\mathrm{i}v_0 k)}{s+\mathrm{i}v_0 k}\right\}\frac{1}{1-\hat{\tilde{\psi}}(k,s)}$$

The MSD is represented by

$$\langle x^2(t)\rangle = \int_{-\infty}^{\infty} x^2\,P(x,t)\,\mathrm{d}x$$
$$\implies \langle \tilde{x}^2(s)\rangle = \frac{\partial^2}{\partial k^2}\hat{\tilde{P}}(k,s)\bigg|_{k=0}$$

The rest of the calculations simply involve substituting all we have gathered together, and using asymptotic analysis to produce tractable results. Using the definitions of $\hat{\tilde{\psi}}(k,s)$ and

$p(x \mid t)$ above, we find

$$\begin{aligned}\hat{\tilde{\psi}}(k,s) &= \frac{1}{2}\int_0^\infty \mathrm{d}t \int_{-\infty}^\infty \mathrm{d}x\, \mathrm{e}^{\mathrm{i}kx-st} \\ &\qquad \times [\delta(-x-t)+\delta(x-t)]w(t) \\ &= \frac{1}{2}\left[\int_0^\infty \mathrm{e}^{-(s+\mathrm{i}k)t}w(t)\,\mathrm{d}t \right. \\ &\qquad \left. + \int_0^\infty \mathrm{e}^{-(s-\mathrm{i}k)t}w(t)\,\mathrm{d}t\right] \\ &= \frac{1}{2}\left[\tilde{w}(s+\mathrm{i}k)+\tilde{w}(s-\mathrm{i}k)\right]\end{aligned}$$

which we will use repeatedly. We will also assume throughout $v_0 = 1$.

When $0 < \gamma < 1$,

$$\begin{aligned}\tilde{w}(s) &= 1-(bs)^\gamma\,\mathrm{e}^{bs}\,\Gamma(1-\gamma,bs) \\ &\simeq 1-(bs)^\gamma\,\Gamma(1-\gamma)\end{aligned}$$

for small s, and therefore (letting $a = b^\gamma\,\Gamma(1-\gamma)$)

$$\begin{aligned}\hat{\tilde{\psi}}(k,s) &= \frac{1}{2}\left[\tilde{w}(s+\mathrm{i}k)+\tilde{w}(s-\mathrm{i}k)\right] \\ &\simeq 1-\frac{1}{2}\left[a(s+\mathrm{i}k)^\gamma + a(s-\mathrm{i}k)^\gamma\right] \\ &\simeq 1-as^\gamma - \frac{a\gamma(1-\gamma)}{2}k^2 s^{\gamma-2}+\ldots\end{aligned}$$

using a general binomial expansion, for $k \to 0$ (small k takes precedence since we are later evaluating this approximation at $k = 0$) and

$$\begin{aligned}\hat{\tilde{\Psi}}(k,s) &= \mathrm{Re}\left\{\frac{a(s+\mathrm{i}k)^\gamma}{s+\mathrm{i}k}\right\} = a\,\mathrm{Re}\left\{(s+\mathrm{i}k)^{\gamma-1}\right\} \\ &= a\left[s^{\gamma-1} - s^{\gamma-3}\frac{(\gamma-1)(\gamma-2)}{2}k^2\right] \\ \implies \hat{\tilde{P}}(k,s) &\simeq \frac{s^{\gamma-1} - s^{\gamma-3}\frac{(\gamma-1)(\gamma-2)}{2}k^2}{s^\gamma - s^{\gamma-2}\frac{\gamma(\gamma-1)}{2}k^2} \\ \implies \langle\tilde{x}^2\rangle &\simeq 2(1-\gamma)s^{-3} \implies \langle x^2\rangle \simeq (1-\gamma)\,t\end{aligned}$$

When $\gamma > 1$, we use the expansion given in [76] for negative z, as $x \to 0^+$,

$$\begin{aligned}\Gamma(z,x) &\sim \Gamma(z) - \sum_{n=0}^\infty (-1)^n \frac{x^{z+n}}{n!(z+n)} \\ \implies \Gamma(1-\gamma,bs) &\sim \Gamma(1-\gamma) - \frac{(bs)^{1-\gamma}}{1-\gamma} \\ &\qquad + \frac{(bs)^{2-\gamma}}{2-\gamma} - \frac{(bs)^{3-\gamma}}{2!(3-\gamma)} + \ldots\end{aligned}$$

wherever $\Gamma(1-\gamma)$ exists (i.e. $\gamma \neq 1, 2, \ldots$). Then the leading order behaviour as $s \to 0$ for $\gamma > 1$ is given by

$$\Gamma(1-\gamma,bs) = -\frac{(bs)^{1-\gamma}}{1-\gamma} + \begin{cases}\Gamma(1-\gamma), & 1<\gamma<2 \\ \frac{(bs)^{2-\gamma}}{2-\gamma}, & \gamma > 2\end{cases}$$

When $1 < \gamma < 2$,

$$\begin{aligned}\Gamma(1-\gamma,bs) &\simeq -\frac{(bs)^{1-\gamma}}{1-\gamma} + \Gamma(1-\gamma) \\ \implies \tilde{w}(s) &= 1-(bs)^\gamma \mathrm{e}^{bs}\Gamma(1-\gamma,bs) \\ &\simeq 1 - \frac{bs}{\gamma-1} - (bs)^\gamma\Gamma(1-\gamma)\end{aligned}$$

For simplicity we rename $\bar{t} = \frac{b}{\gamma-1}$ and $c = -b^\gamma\Gamma(1-\gamma)$ to obtain

$$\tilde{w}(s) = 1 - s\bar{t} + cs^\gamma \quad \text{as} \quad s \to 0$$

The first expression is especially natural since $\bar{t}$ is precisely the mean of the Pareto waiting time $\bar{t} = \mathbb{E}[w(t)]$, and the second is also reasonable since $\Gamma(1-\gamma)$ is negative. Then

$$\begin{aligned}\hat{\tilde{\psi}}(k,s) &= \frac{1}{2}\left[\tilde{w}(s+\mathrm{i}k)+\tilde{w}(s-\mathrm{i}k)\right] \\ &\simeq 1 - s\bar{t} + cs^\gamma - cb^2k^2s^{\gamma-2}+\ldots\end{aligned}$$

using $b^2 = \frac{\gamma(\gamma-1)}{2}$. Then

$$\begin{aligned}\hat{\tilde{\Psi}}(k,s) &= \mathrm{Re}\left\{\frac{\bar{t}(s+\mathrm{i}k) - c(s+\mathrm{i}k)^\gamma}{s+\mathrm{i}k}\right\} \\ &= \bar{t} - c\,\mathrm{Re}\left\{(s+\mathrm{i}k)^{\gamma-1}\right\} \\ &= \bar{t} - c\left[s^{\gamma-1} - s^{\gamma-3}\frac{(\gamma-1)(\gamma-2)}{2}k^2\right] \\ \implies \hat{\tilde{P}}(k,s) &= \frac{\bar{t} - c\left[s^{\gamma-1} - s^{\gamma-3}\frac{(\gamma-1)(\gamma-2)}{2}k^2\right]}{s\bar{t} - cs^\gamma + cs^{\gamma-2}\frac{\gamma(\gamma-1)}{2}k^2} \\ \implies \langle\tilde{x}^2\rangle &= \frac{2cs^{\gamma-3}(\gamma-1)}{s\bar{t}-cs^\gamma} \to \frac{2c(\gamma-1)}{\bar{t}}s^{\gamma-4} \\ &= 2b^{\gamma-1}\Gamma(2-\gamma)(\gamma-1)s^{\gamma-4} \\ \implies \langle x^2\rangle &= 2b^{\gamma-1}\frac{\Gamma(2-\gamma)}{\Gamma(4-\gamma)}(\gamma-1)\,t^{3-\gamma} \\ &= \frac{2b^{\gamma-1}(\gamma-1)}{(3-\gamma)(2-\gamma)}\,t^{3-\gamma}\end{aligned}$$

When $\gamma > 2$,

$$\begin{aligned}\Gamma(1-\gamma,bs) &\simeq -\frac{(bs)^{1-\gamma}}{1-\gamma} + \frac{(bs)^{2-\gamma}}{2-\gamma} \\ \implies \tilde{w}(s) &= 1-(bs)^\gamma \mathrm{e}^{bs}\Gamma(1-\gamma,bs) \\ &\simeq 1 - \left[\frac{bs}{\gamma-1} - \frac{(bs)^2}{\gamma-2}\right] \\ &\qquad \times \left(1 + bs + \frac{(bs)^2}{2} + \ldots\right) \\ &\simeq 1 - \frac{bs}{\gamma-1} - \left[\frac{1}{\gamma-1} - \frac{1}{\gamma-2}\right](bs)^2 + \ldots \\ &= 1 - \frac{bs}{\gamma-1} + \frac{(bs)^2}{(\gamma-1)(\gamma-2)} + \ldots\end{aligned}$$

to leading order, and so letting $a = (\gamma-1)^{-1}$,

$$\begin{aligned}\hat{\tilde{\psi}}(s) &= 1 - abs + \frac{a^2}{1-a}\frac{b^2}{2}[(s+\mathrm{i}k)^2 + (s-\mathrm{i}k)^2] \\ &= 1 - abs + \frac{a^2}{1-a}\, b^2\,(s^2-k^2)\end{aligned}$$

and therefore we find

$$\begin{aligned}\hat{\tilde{\Psi}}(k,s) &= \mathrm{Re}\left\{\frac{ab(s+\mathrm{i}k) - \frac{a^2}{1-a}b^2(s+\mathrm{i}k)^2}{s+\mathrm{i}k}\right\} \\ &= ab - \frac{a^2}{1-a}b^2 s \\ \implies \hat{\tilde{P}}(k,s) &= \frac{ab - \frac{a^2}{1-a}b^2 s}{abs - \frac{a^2}{1-a}b^2(s^2-k^2)} \\ \implies \langle\tilde{x}^2\rangle &= \frac{2ab}{s^2(1-a-abs)} \to 2\frac{a}{1-a}bs^{-2} \\ \implies \langle x^2\rangle &= 2\frac{a}{1-a}\,bt = \frac{2b}{\gamma-2}\,t\end{aligned}$$

In conclusion, we find to leading order

$$\langle x^2\rangle \sim \begin{cases} \frac{2b}{\gamma-2}\,t, & \gamma > 2 \\ \frac{2b^{\gamma-1}(\gamma-1)}{(3-\gamma)(2-\gamma)}\,t^{3-\gamma}, & 1<\gamma<2 \\ (1-\gamma)\,t^2, & \gamma<1 \end{cases}$$

and therefore

$$K(z) := \lim_{t\to\infty}\frac{\langle x^2\rangle}{t^\beta} = \begin{cases} \frac{2b}{\gamma-2}, & 1<z<\frac{3}{2} \\ \frac{2b^{\gamma-1}(\gamma-1)}{(3-\gamma)(2-\gamma)}, & \frac{3}{2}<z<2 \\ 1-\gamma, & z>2 \end{cases}$$

[1] A. Bunde, J. Caro, J. Kärger, and G. Vogl, eds., *Diffusive Spreading in Nature, Technology and Society* (Springer, Berlin, 2018).
[2] K. Pearson, Nature **72**, 294, 342 (1905).
[3] A. Einstein, Annalen der Physik **19**, 289 (1906).
[4] J. Bouchaud and A. Georges, Phys. Rep. **195**, 127 (1990).
[5] W. Coffey, Y. P. Kalmykov, and J. T. Waldron, *The Langevin Equation* (World Scientific, Singapore, 2004).
[6] R. Klages, G. Radons, and I. M. Sokolov, eds., *Anomalous transport: Foundations and Applications* (Wiley-VCH, Berlin, 2008).
[7] R. Metzler and J. Klafter, Phys. Rep. **339**, 1 (2000).
[8] R. Metzler, J.-H. Jeon, A. Cherstvy, and E. Barkai, Phys. Chem. Chem. Phys. **16**, 24128 (2014).
[9] F. Höfling and T. Franosch, Rep. Prog. Phys. **76**, 046602/1 (2013).
[10] V. Zaburdaev, S. Denisov, and J. Klafter, Rev. Mod. Phys. **87**, 483 (2015).
[11] D. Evans and G. Morriss, *Statistical mechanics of nonequilibrium liquids* (Academic Press, London, 1990).
[12] W. Hoover, *Time reversibility, computer simulation, and chaos* (World Scientific, Singapore, 1999).
[13] P. Gaspard, *Chaos, scattering and statistical mechanics* (Cambridge University Press, Cambridge, UK, 1998).
[14] J. R. Dorfman, *An introduction to chaos in nonequilibrium statistical mechanics*, Cambridge Lecture Notes in Physics No. 14 (Cambridge University Press, Cambridge, UK, 1999).
[15] G. Zaslavsky, Phys. Rep. **371**, 461 (2002).
[16] R. Klages, *Microscopic chaos, fractals and transport in nonequilibrium statistical mechanics*, Advanced Series in Nonlinear Dynamics, Vol. 24 (World Scientific, Singapore, 2007).
[17] P. Castiglione, M. Falcioni, A. Lesne, and A. Vulpiani, *Chaos and Coarse Graining in Statistical Mechanics* (Cambridge University Press, Cambridge, 2008).
[18] H. Fujisaka and S. Grossmann, Z. Physik B **48**, 261 (1982).
[19] M. Schell, S. Fraser, and R. Kapral, Phys. Rev. A **26**, 504 (1982).
[20] T. Geisel and J. Nierwetberg, Phys. Rev. Lett. **48**, 7 (1982).
[21] T. Geisel and S. Thomae, Phys. Rev. Lett. **52**, 1936 (1984).
[22] M. Shlesinger and J. Klafter, Phys. Rev. Lett. **54**, 2551 (1985).
[23] T. Geisel, J. Nierwetberg, and A. Zacherl, Phys. Rev. Lett. **54**, 616 (1985).
[24] G. Zumofen and J. Klafter, Phys. Rev. E **47**, 851 (1993).
[25] G. Zumofen and J. Klafter, Physica D **69**, 436 (1993).
[26] R. Klages and J. R. Dorfman, Phys. Rev. Lett. **74**, 387 (1995).
[27] R. Klages and J. Dorfman, Phys. Rev. E **55**, R1247 (1997).
[28] E. Barkai and J. Klafter, Phys. Rev. Lett. **79**, 2245 (1997).
[29] R. Klages and J. R. Dorfman, Phys. Rev. E **59**, 5361 (1999).
[30] R. Klages and N. Korabel, J. Phys. A **35**, 4823 (2002).
[31] E. Barkai, Phys. Rev. Lett. **90**, 104101/1 (2003).
[32] N. Korabel, A. Chechkin, R. Klages, I. Sokolov, and V. Gonchar, Europhys. Lett. **70**, 63 (2005).
[33] N. Korabel, R. Klages, A. Chechkin, I. Sokolov, and V. Gonchar, Phys. Rev. E **75**, 036213 (2007).
[34] T. Albers, D. Müller-Bender, L. Hille, and G. Radons, Phys. Rev. Lett. **128**, 074101 (2022).
[35] R. Artuso, Phys. Lett. A **160**, 528 (1991).
[36] R. Artuso, G. Casati, and R. Lombardi, Phys. Rev. Lett. **71**, 62 (1993).
[37] C. Dettmann and P. Cvitanovic, Phys. Rev. E **56**, 6687 (1997).
[38] C. Dettmann and P. Dahlqvist, Phys. Rev. E **57**, 5303 (1998).
[39] P. Cvitanović, R. Artuso, R. Mainieri, G. Tanner, and G. Vattay, *Chaos: Classical and quantum* (Niels Bohr Institute, Copenhagen, 2007) webbook under chaosbook.org.
[40] X.-J. Wang and C.-K. Hu, Phys. Rev. E **48**, 728 (1993).
[41] R. Stoop, W.-H. Steeb, and G. Radons, Phys. Lett. A **202**, 195 (1995).
[42] J. Groeneveld and R. Klages, J. Stat. Phys. **109**, 821 (2002).
[43] N. Korabel and R. Klages, Phys. Rev. Lett. **89**, 214102/1 (2002).
[44] S. Tasaki and P. Gaspard, Physica D **187**, 51 (2004).
[45] P. Gaspard and X.-J. Wang, Proc. Natl. Acad. Sci. USA **85**, 4591 (1988).
[46] G. Zaslavsky and D. Usikov, *Weak chaos and quasi-regular patterns*, Cambridge Nonlinear Science Series (Cambridge University Press, Cambridge, 2001).

[47] R. Klages, in *From Hamiltonian chaos to complex systems*, edited by X. Leoncini and M. Leonetti (Springer, Berlin, 2013) pp. 3–42.
[48] P. Manneville and Y. Pomeau, Phys. Lett. A **75**, 1 (1979).
[49] P. Manneville, J. Physique **41**, 1235 (1980).
[50] Y. Pomeau and P. Manneville, Commun. Math. Phys. **74**, 189 (1980).
[51] A. Schulz, *Parameter-dependent deterministic diffusion in intermittent Pomeau-Manneville maps*, Master's thesis, Technische Universität Dresden, Dresden, Germany (2020).
[52] D. Pegler, *Anomalous diffusion in weakly chaotic systems*, Master's thesis, Queen Mary, University of London, London, UK (2017).
[53] R. Klages, *Deterministic diffusion in one-dimensional chaotic dynamical systems*, Doctoral thesis, Technische Universität Berlin, Berlin, Germany (1995).
[54] J. Klafter and I. Sokolov, *First steps in random walks: from tools to applications* (Oxford University Press, New York, 2011).
[55] E. Montroll and G. Weiss, J. Math. Phys. **6**, 167 (1965).
[56] E. Montroll and H. Scher, J. Stat. Phys. **9**, 101 (1973).
[57] H. Scher and E. Montroll, Phys. Rev. B **12**, 2455 (1975).
[58] M. Shlesinger, J. Klafter, and Y. Wong, J. Stat. Phys. **27**, 499 (1982).
[59] J. Klafter, A. Blumen, and M. Shlesinger, Phys. Rev. A **35**, 3081 (1987).
[60] M. Shlesinger, B. West, and J. Klafter, Phys. Rev. Lett. **58**, 1100 (1987).
[61] R. Kubo, Rep. Prog. Phys. **29**, 255 (1966).
[62] G. I. Taylor, Proc. London Math. Soc. **s2-20**, 196 (1922).
[63] G. Knight and R. Klages, Phys. Rev. E **84**, 041135/1 (2011).
[64] V. Zaburdaev, I. Fouxon, S. Denisov, and E. Barkai, Phys. Rev. Lett. **117**, 270601 (2016).
[65] T. Akimoto and E. Barkai, Phys. Rev. E **87**, 032915 (2013).
[66] M. Thaler, Israel Journal of Mathematics **46**, 67 (1983).
[67] R. Zweimüller, Nonlinearity **11**, 1263 (1998).
[68] M. Thaler, Studia Mathematica **143**, 103 (2000).
[69] J. Bouchaud, J. Phys. I **2**, 1705 (1992).
[70] E. Barkai and G. Margolin, Israel Journal of Chemistry **44**, 353 (2004).
[71] R. Metzler, J.-H. Jeon, A. G. Cherstvy, and E. Barkai, Phys. Chem. Chem. Phys. **16**, 24128 (2014).
[72] R. Metzler, J.-H. Jeon, A. G. Cherstvy, and E. Barkai, Phys. Chem. Chem. Phys. **16**, 24128 (2014).
[73] F. Stefani, J. Hoogenboom, and E. Barkai, Phys. Tod. **62**, 34 (2009).
[74] E. Lutz and F. Renzoni, Nature Physics **9**, 615 (2013).
[75] L. Salari, L. Rondoni, C. Giberti, and R. Klages, Chaos **25**, 073133/1 (2015).
[76] C. Bender and S. Orszag, *Asymptotic methods and perturbation theory*, Advanced Mathematical Methods for Scientists and Engineers, Vol. I (Springer, New York, 1978).